


 Cite this: *RSC Adv.*, 2020, 10, 37023

 Received 3rd September 2020  
 Accepted 29th September 2020

DOI: 10.1039/d0ra07575b

[rsc.li/rsc-advances](http://rsc.li/rsc-advances)

# Deep eutectic solvent in water pickering emulsions stabilised by cellulose nanofibrils†‡

 Saffron J. Bryant,<sup>ID</sup>\*<sup>ab</sup> Marcelo A. da Silva,<sup>ID</sup><sup>a</sup> Kazi M. Zakir Hossain,<sup>a</sup> Vincenzo Calabrese,<sup>a</sup> Janet L. Scott<sup>ID</sup><sup>ac</sup> and Karen J. Edler<sup>ID</sup>\*<sup>a</sup>

Deep eutectic solvent (menthol : dodecanoic acid) in water (30 : 70) emulsions stabilised with partially oxidised cellulose nanoparticles remained stable for 200 days at room temperature. Deep eutectic-based emulsions offer potential for non-aqueous reaction systems, chemical extraction, and controlled release. Pickering emulsions using polysaccharides are less toxic and more stable than surfactant-stabilised emulsions.

## Introduction

Deep eutectic solvents (DESs) are a promising new type of non-volatile solvent composed of hydrogen bond donors and acceptors. They are a highly tuneable subclass of ionic liquid (IL) but are often cheaper, easier to make, and more environmentally friendly.<sup>1–4</sup>

DESs and the broader ionic liquid (IL) solvent class have potential as reaction media and reactor systems.<sup>2,5–9</sup> Their tuneable properties, including temperature stability and solvation of drug and catalytic molecules make ILs and DESs preferable to traditional oil/water emulsions.<sup>2,10,11</sup> There have been some reports of ionic liquid (IL) based emulsions (using IL as an additive, or as the oil, or as the polar phase, or even IL in IL emulsions).<sup>10–13</sup> There are also reports of DES in oil emulsions, stabilised with conventional surfactants.<sup>14</sup> However, to the authors' knowledge, the only report of a DES in water emulsion comes from the commercial EMLA® cream (EMLA stands for Eutectic Mixture of Local Anesthetics) which uses a eutectic mixture of lidocaine and prilocaine, stabilised by a non-ionic surfactant.<sup>15</sup>

The DES in water pickering emulsion reported here has an advantage over these previously reported formulations because it does not use expensive and potentially toxic surfactants. In addition, as water is the major phase, it is more compatible with

applications that require low toxicity and low cost, than DES in oil emulsions.

Menthol : dodecanoic acid (2 : 1) is a hydrophobic DES with a melting point around 7 °C.<sup>16</sup> It has potential for extraction of materials from water,<sup>17,18</sup> separation of metals,<sup>19,20</sup> and extraction of pesticides from water.<sup>21</sup>

TEMPO-oxidised cellulose nanofibrils (OCNF) are negatively charged nanoparticles that can form Pickering-type emulsions.<sup>22–24</sup> Pickering emulsions stabilised by other polysaccharide-based nanoparticles have also been reported.<sup>25–27</sup> However, until now, their use has been limited to emulsions using model oils (such as hexadecane), or sunflower oil.

Emulsions containing 30 vol% menthol : dodecanoic acid were stabilised using either OCNF, or hydrophobically modified OCNF (C8-OCNF). These emulsions, including their stability over time were assessed using laser diffraction, visual observation, and small-angle X-ray scattering.

## Experimental

### Oxidised cellulose nanofibrils

Oxidised cellulose nanofibrils provided by Croda® as a *ca.* 8 wt% solids paste in water were prepared *via* TEMPO-mediated oxidation as previously described.<sup>28,29</sup> Previous work by this group determined the degree of oxidation for this particular batch of fibrils to be 25% *i.e.* number of carboxylate groups compared to total anhydroglucose units.<sup>30,31</sup> The fibrils have a large aspect ratio (hundreds of nm in length and a cross section of ~5 nm)<sup>32</sup> and a high negative surface charge (–60 mV in  $\zeta$  potential).<sup>28–30</sup>

Residual salts and preservatives were removed from OCNF by dialysis against deionised water (18.2 M $\Omega$  cm) as previously described.<sup>32</sup> The OCNF was then freeze-dried and resuspended to 1.5 wt% in deionised water before being dispersed by sonication (Ultrasonic Processor, FB-505, Fisher – 550 W), at 30%

<sup>a</sup>Department of Chemistry, University of Bath, Claverton Down, Bath, BA2 7AY, UK. E-mail: K.Edler@bath.ac.uk

<sup>b</sup>School of Science, RMIT University, Melbourne, Victoria, 3001, Australia. E-mail: saffron.bryant@rmit.edu.au

<sup>c</sup>Centre for Sustainable Chemical Technologies, University of Bath, Claverton Down, Bath, BA2 7AY, UK

† Data supporting this work are freely accessible in the Bath research data archive system at DOI: 10.15125/BATH-00920.<sup>44</sup>

‡ Electronic supplementary information (ESI) available. See DOI: 10.1039/d0ra07575b



amplitude with 1 s on 1 s off pulses, for ~1 h or until the dispersion became transparent.

### Hydrophobic modification

OCNF fibrils were prepared as described above and dispersed at ~0.5 wt% in water *via* probe sonication. Octylamine (Arcos Organic, +99%) was added in large excess (~10×) and the pH corrected to 5 (with diluted hydrochloric acid solution, *ca.* 1 M). An equimolar amount of EDC (1-ethyl-3-(3-dimethylaminopropyl)carbodiimide hydrochloride) (Sigma, +99%)/NHS (*N*-hydroxysuccinimide) (Sigma, 98%) 1 : 1 solution was added dropwise and the pH of the mixture maintained at pH 5.

The reaction was left overnight and then 50 wt% propan-2-ol (BDH Chemicals, 100%) in water was added to the reaction mixture in a 2 to 1 ratio which causes the C8-OCNF to aggregate. The mixture was centrifuged at 5000 RCF (relative centrifugal force) for ten minutes and the precipitate (C8-OCNF) collected. The precipitate was washed twice more with 50 wt% propan-2-ol and centrifuged.

The precipitate was re-suspended in deionised water and dialysed against deionised water for 24 h to remove the propan-2-ol. The C8-OCNF was dialysed for a further 24 h against deionised water with a pH of 3 to remove any ionically bound amine. Further dialysis was performed against neutral deionised water for 72 h with regular replacement of the water to remove any remaining salts.

As with OCNF, the C8-OCNF was then freeze-dried and re-dispersed to the desired wt% using sonication.

The  $\zeta$ -potential of C8-OCNF was measured using a Malvern Zeta-sizer Nano ZSP® (Malvern, UK) in a folded capillary electrode cell using ultrapure Milli-Q water as the dispersant. The sample was equilibrated at 25 °C for 120 s prior to testing and the results taken from an average of 3 measurements of 100 scans each.

### Starch

Starch dispersions were prepared by dissolving 1.5 wt% soluble starch (Sigma-Aldrich, S9765) in deionised water at 80 °C with stirring for 45 minutes, then allowing it to return to room temperature.

### Deep eutectic solvent

Menthol (Alfa Aesar, 99%) and dodecanoic acid (Acros, 98%) were combined in a 2 : 1 molar ratio and stirred at 50 °C until a homogenous liquid was formed.

### Emulsions

Aqueous dispersions were combined with the DES in a 70 : 30 volume ratio and then the samples were sonicated (Ultrasonic Processor, FB-505, Fisher – 550 W), at 20% amplitude with 1 s on 1 s off pulses, for 2 minutes. For polysaccharide-stabilised emulsions, the aqueous phase contained either starch (Sigma, Soluble S9765), OCNF or C8-OCNF at 1.5 wt%. For the surfactant-stabilised emulsions, the aqueous phase contained

either 1 wt% Tween20 (8 mM) (Sigma) or 100 mM AOT (Acros, 96%) (4.5 wt%).

### Characterisation

Droplet measurements were made using a Mastersizer 3000E laser diffraction particle size analyser (Malvern, UK). Samples were added dropwise to the dispersion unit until the obscuration was within the acceptable range (7–20%). Five repeat measurements were made for each time point to ensure sample stability. Droplet size is reported as Sauter diameter  $D[3,2]$  for easy comparison.

SAXS measurements were performed on an Anton-Paar SAXSpot 2.0 provided by the Material and Chemical Characterisation Facility (MC<sup>2</sup>)<sup>33</sup> equipped with a copper source (Cu K $\alpha$ ,  $\lambda = 1.542 \text{ \AA}$ ) and a 2D EIGER R series Hybrid Photon Counting (HPC) detector. The sample detector distance was 556.9 mm covering a  $q$  range of about 0.008–0.4  $\text{\AA}^{-1}$ . The emulsions were loaded into 1 mm quartz capillaries and measured at 25 °C ( $\pm 0.1$  °C Peltier unit). Data was collected in one frame, with 900 s exposure, then processed. Fitting was performed using SASView (Version 4.2.1, see <http://www.sasview.org/> for more information). The model for elliptical cylinders was used from SASView 4.2.1 without modification.<sup>34</sup> Fitting parameters are given in the ESI.†

Viscosity of 1.5 wt% OCNF or C8-OCNF in water was measured using a stress-controlled Discovery Hybrid Rheometer, Model HR-3 (TA Instruments) with a sand-blasted 40 mm parallel plate geometry with a gap of ~800  $\mu\text{m}$ . Flow sweeps were performed at shear rates from 0.01 to 100  $\text{s}^{-1}$  with ten points per decade, at 25 °C (Peltier unit,  $\pm 0.1$  °C).

## Results and discussion

Emulsions made with OCNF remained visually stable for more than 200 days at room temperature with no evidence of aggregation or creaming (Fig. 1). Emulsions made with C8-OCNF creamed after 23 days, but the creamed layer remained stable (see Fig. S1†). Creaming is due to the lower density of the DES droplets, compared to the bulk water.

Visual observations were supported by laser diffraction measurements of droplet size. As shown in Fig. 2, droplets stabilised by OCNF remained stable in excess of 200 days with only a minor increase in droplet size. Droplets stabilised with C8-OCNF were smaller and appeared to be more stable, with almost no change even after 100 days.

The hydrophobic chains on C8-OCNF will allow greater interaction with the hydrophobic DES, compared to unmodified



Fig. 1 DES in water emulsion (30 : 70 volume ratio) stabilised by 1.5 wt% OCNF after more than 200 days at room temperature.



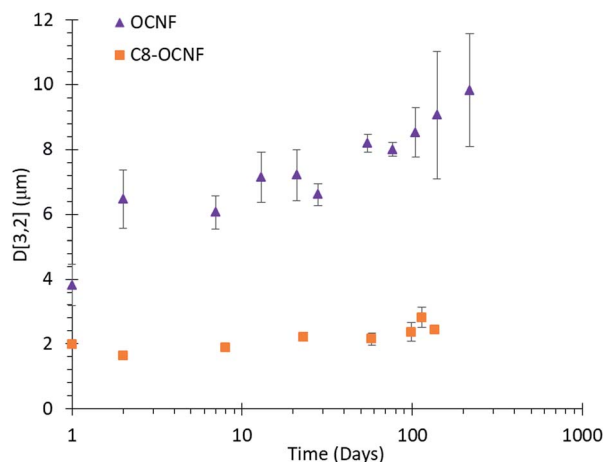


Fig. 2 Average droplet size of DES in water (30 : 70 volume ratio) emulsions stabilised with either 1.5 wt% OCNF or C8-OCNF, error bars based on standard deviation of repeat measurements.

OCNF, and reduce the energy necessary to create a new interface, thus improving homogenization. This could allow tighter packing around the droplets, leading to smaller, more stable droplets. Similar effects have been observed for cellulose nanocrystal-stabilised emulsions using standard oils.<sup>35,36</sup>

While larger droplets may be expected to cream faster due to having a lower density, this was not the case here. The difference in creaming between OCNF and C8-OCNF is due to the higher viscosity of the continuous phase of OCNF- over C8-OCNF-stabilised emulsions which works to prevent creaming (Fig. S2†).<sup>22</sup> Increased viscosity comes from the higher surface charge of OCNF compared to C8-OCNF, which increases the excluded volume.

Previous emulsion research demonstrated that cellulose nanofibrils with higher charge provided greater stability than lower charged fibrils.<sup>23</sup> The method of hydrophobisation used here necessitates the replacement of some of the negative carboxylate groups with hydrophobic chains, thus reducing the  $\zeta$  potential from  $-60$  mV to  $-43$  mV. This would reduce repulsion between fibrils, and allow movement of droplets, ultimately leading to creaming.

In comparison, emulsions stabilised with soluble starch polymers, rather than cellulose particles, which have an even smaller  $\zeta$  potential ( $-14 \pm 1$  mV)<sup>37</sup> creamed on day 2. By day 23 there was precipitation and clumping and the mean droplet size was over  $20 \mu\text{m}$  (Fig. S3†).

Small angle X-ray scattering (SAXS) was used to investigate the structure of these emulsions. Fig. 3 shows the scattering patterns for OCNF and C8-OCNF in water and for the DES in water emulsions.

The scattering pattern of OCNF in water can be fit with an elliptical cylinder model with a minor radius of  $12.4 \pm 2 \text{ \AA}$  and a major radius of  $58 \pm 9 \text{ \AA}$ , in line with previous research.<sup>32</sup> The same model can be used to fit the majority of the data for the emulsion sample, with a minor radius ( $13.4 \pm 2 \text{ \AA}$ ) and a major radius ( $66 \pm 9 \text{ \AA}$ ) that are within the error for OCNF fibrils in

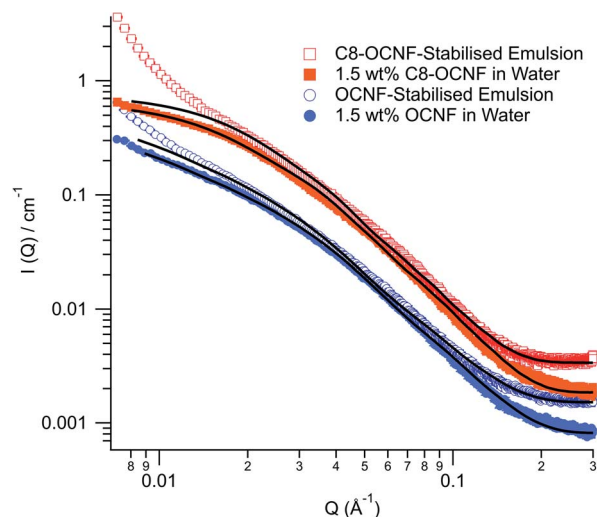


Fig. 3 SAXS patterns of 1.5 wt% OCNF (filled circles) or C8-OCNF (filled squares) in water, and the DES in water emulsions stabilised by either 1.5 wt% OCNF (open circles) or C8-OCNF (open squares). Model fits are shown as black lines (parameters given in ESI†).

water, suggesting that the OCNF fibrils are dominating the SAXS signal.

The scattering pattern for C8-OCNF in water can be fit with the same parameters as OCNF except that the length is significantly shorter ( $300 \pm 20$  compared to  $>1000 \text{ \AA}$ ). Given the benign nature of the modification procedure, this apparent change in length is most likely a result of fibril flocs. The length reported by SAXS is actually the distance between intersection points rather than an actual shortening of the fibrils (see Fig. S5†). Similar aggregation has been observed for nanocrystalline cellulose upon addition of salt to screen repulsive charges.<sup>38</sup> As with OCNF, the SAXS data from the emulsion stabilised by C8-OCNF can be fit with a similar model.

As shown in Fig. 3, the scattering from both emulsion samples have an upturn at low  $q$  which cannot be fitted with the elliptical cylinder model. This is probably from the emulsion droplets. Based on the laser diffraction data, these droplets are far outside of the probed range of this SAXS instrument and so cannot be fitted. The upturn appears to happen at higher  $q$  for the C8-OCNF stabilised emulsions, indicative of smaller droplets, which is consistent with the laser diffraction results. Also, due to the smaller surface charge, C8-OCNF is prone to self-aggregation, which could also contribute to the low- $q$  signal.

The SAXS results demonstrate that for both OCNF and C8-OCNF the cellulose nanofibril structure is unchanged in the presence of the hydrophobic DES, compared to in water dispersions.

For the purposes of completeness, DES in water emulsions were also made with more traditional surfactants (dioctyl sodium sulfosuccinate (AOT) or Tween20). This produced emulsions with even smaller droplets ( $\sim 0.2\text{--}0.6 \mu\text{m}$ ) that remained stable for more than 60 days (see ESI†). However, the emulsion stabilised with AOT broke down by day 100, with separate oil and water layers. The emulsion stabilised with





- 17 C. Florindo, L. C. Branco and I. M. Marrucho, Quest for Green-Solvent Design: From Hydrophilic to Hydrophobic (Deep) Eutectic Solvents, *ChemSusChem*, 2019, **12**(8), 1549–1559.
- 18 R. Verma and T. Banerjee, Liquid–Liquid Extraction of Lower Alcohols Using Menthol-Based Hydrophobic Deep Eutectic Solvent: Experiments and COSMO-SAC Predictions, *Ind. Eng. Chem. Res.*, 2018, **57**(9), 3371–3381.
- 19 N. Schaeffer, M. A. R. Martins, C. M. S. S. Neves, S. P. Pinho and J. A. P. Coutinho, Sustainable hydrophobic terpene-based eutectic solvents for the extraction and separation of metals, *Chem. Commun.*, 2018, **54**(58), 8104–8107.
- 20 E. E. Tereshatov, M. Y. Boltoeva and C. M. Folden, First evidence of metal transfer into hydrophobic deep eutectic and low-transition-temperature mixtures: indium extraction from hydrochloric and oxalic acids, *Green Chem.*, 2016, **18**(17), 4616–4622.
- 21 C. Florindo, L. C. Branco and I. M. Marrucho, Development of hydrophobic deep eutectic solvents for extraction of pesticides from aqueous environments, *Fluid Phase Equilib.*, 2017, **448**, 135–142.
- 22 M. Gestranus, P. Stenius, E. Kontturi, J. Sjöblom and T. Tammelinn, Phase behaviour and droplet size of oil-in-water Pickering emulsions stabilised with plant-derived nanocellulosic materials, *Colloids Surf., A*, 2017, **519**, 60–70.
- 23 R. Aaen, F. W. Brodin, S. Simon, E. B. Heggset and K. Syverud, Oil-in-Water Emulsions Stabilized by Cellulose Nanofibrils—The Effects of Ionic Strength and pH, *Nanomaterials*, 2019, **9**(2), 259.
- 24 S. U. Pickering, CXCVI.—Emulsions, *J. Chem. Soc. Trans.*, 1907, **91**, 2001–2021.
- 25 L. Bai, S. Huan, W. Xiang and O. J. Rojas, Pickering emulsions by combining cellulose nanofibrils and nanocrystals: phase behavior and depletion stabilization, *Green Chem.*, 2018, **20**(7), 1571–1582.
- 26 F. Cherhal, F. Cousin and I. Capron, Structural Description of the Interface of Pickering Emulsions Stabilized by Cellulose Nanocrystals, *Biomacromolecules*, 2016, **17**(2), 496–502.
- 27 M. M. Kasprzak, W. Macnaughtan, S. Harding, P. Wilde and B. Wolf, Stabilisation of oil-in-water emulsions with non-chemical modified gelatinised starch, *Food Hydrocolloids*, 2018, **81**, 409–418.
- 28 T. Saito, Y. Nishiyama, J.-L. Putaux, M. Vignon and A. Isogai, Homogeneous Suspensions of Individualized Microfibrils from TEMPO-Catalyzed Oxidation of Native Cellulose, *Biomacromolecules*, 2006, **7**(6), 1687–1691.
- 29 A. Isogai, T. Saito and H. Fukuzumi, TEMPO-oxidized cellulose nanofibers, *Nanoscale*, 2011, **3**(1), 71–85.
- 30 J. C. Courtenay, M. A. Johns, F. Galembeck, C. Deneke, E. M. Lanzoni, C. A. Costa, J. L. Scott and R. I. Sharma, Surface modified cellulose scaffolds for tissue engineering, *Cellulose*, 2017, **24**(1), 253–267.
- 31 V. Calabrese, M. A. da Silva, J. Schmitt, J. C. Muñoz-Garcia, V. Gabrielli, J. L. Scott, J. Angulo, Y. Z. Khimyak and K. J. Edler, Surfactant controlled zwitterionic cellulose nanofibril dispersions, *Soft Matter*, 2018, **14**(38), 7793–7800.
- 32 J. Schmitt, V. Calabrese, M. A. da Silva, S. Lindhoud, V. Alfredsson, J. L. Scott and K. J. Edler, TEMPO-oxidised cellulose nanofibrils; probing the mechanisms of gelation via small angle X-ray scattering, *Phys. Chem. Chem. Phys.*, 2018, **20**(23), 16012–16020.
- 33 Material and Chemical Characterisation Facility (MC<sup>2</sup>), DOI: 10.15125/mx6j-3r54.
- 34 L. A. Feigin; D. I. Svergun, *Structure Analysis by Small-Angle X-Ray and Neutron Scattering*. Springer US: 1987; p. 335.
- 35 M. E. H. v. d. Berg, S. Kuster, E. J. Windhab, L. M. C. Sagis and P. Fischer, Nonlinear shear and dilatational rheology of viscoelastic interfacial layers of cellulose nanocrystals, *Phys. Fluids*, 2018, **30**(7), 072103.
- 36 M. E. H. van den Berg, S. Kuster, E. J. Windhab, J. Adamcik, R. Mezzenga, T. Geue, L. M. C. Sagis and P. Fischer, Modifying the Contact Angle of Anisotropic Cellulose Nanocrystals: Effect on Interfacial Rheology and Structure, *Langmuir*, 2018, **34**(37), 10932–10942.
- 37 K. M. Z. Hossain, V. Calabrese, M. A. da Silva, S. J. Bryant, J. Schmitt, J. L. Scott and K. J. Edler, Cationic surfactants as a non-covalent linker for oxidised cellulose nanofibrils and starch-based hydrogels, *Carbohydr. Polym.*, 2020, **233**, 115816.
- 38 P. Bertsch, A. Sánchez-Ferrer, M. Bagnani, S. Isabettni, J. Kohlbrecher, R. Mezzenga and P. Fischer, Ion-Induced Formation of Nanocrystalline Cellulose Colloidal Glasses Containing Nematic Domains, *Langmuir*, 2019, **35**(11), 4117–4124.
- 39 B. P. Binks, Particles as surfactants—similarities and differences, *Curr. Opin. Colloid Interface Sci.*, 2002, **7**(1), 21–41.
- 40 G. Lagaly, M. Reese and S. Abend, Smectites as colloidal stabilizers of emulsions: I. Preparation and properties of emulsions with smectites and nonionic surfactants, *Appl. Clay Sci.*, 1999, **14**(1), 83–103.
- 41 S. Abend, N. Bonnke, U. Gutschner and G. Lagaly, Stabilization of emulsions by heterocoagulation of clay minerals and layered double hydroxides, *Colloid Polym. Sci.*, 1998, **276**(8), 730–737.
- 42 R. J. Crawford, K. J. Edler, S. Lindhoud, J. L. Scott and G. Unali, Formation of shear thinning gels from partially oxidised cellulose nanofibrils, *Green Chem.*, 2012, **14**(2), 300–303.
- 43 J. L. Scott; C. Smith and G. Unali, *Aqueous Gels*, WO2012171725, 2012.
- 44 S. Bryant, M. Alves Da Silva, Z. Hossain, V. Calabrese, J. Scott and K. Edler, *Dataset for “Deep Eutectic Solvent in Water Pickering Emulsions Stabilised by Cellulose Nanofibrils”*, Bath: University of Bath Research Data Archive, 2020, DOI: 10.15125/BATH-00920.

